J Physiol 590.7 (2012) pp 1599–1614

The Journal of Physiology

Altered Kv3.3 channel gating in early-onset spinocerebellar ataxia type 13

Natali A. Minassian[1], Meng-Chin A. Lin[1] and Diane M. Papazian[1,2,3]

[1]Department of Physiology, [2]Molecular Biology Institute and [3]Brain Research Institute, David Geffen School of Medicine, University of California at Los Angeles, Los Angeles, CA 90095-1751, USA

Key points

- Mutations in the Kv3.3 voltage-gated potassium channel cause the human genetic disease spinocerebellar ataxia type 13.
- Depending on the mutation, the disease emerges during early childhood or during adulthood.
- Kv3.3 mutations affect channel function but previous work did not clarify the relationship between changes in channel activity and the age of disease onset.
- In this study, we showed that mutations that cause early-onset disease have similar effects on the voltage dependence and kinetics of channel opening, whereas a mutation that causes adult-onset disease reduces current amplitude but has little effect on voltage dependence or kinetics.
- We conclude that changes in channel gating contribute substantially to an early age of onset in spinocerebellar ataxia type 13.

Abstract Mutations in Kv3.3 cause spinocerebellar ataxia type 13 (SCA13). Depending on the causative mutation, SCA13 is either a neurodevelopmental disorder that is evident in infancy or a progressive neurodegenerative disease that emerges during adulthood. Previous studies did not clarify the relationship between these distinct clinical phenotypes and the effects of SCA13 mutations on Kv3.3 function. The F448L mutation alters channel gating and causes early-onset SCA13. R420H and R423H suppress Kv3 current amplitude by a dominant negative mechanism. However, R420H results in the adult form of the disease whereas R423H produces the early-onset, neurodevelopmental form with significant clinical overlap with F448L. Since individuals with SCA13 have one wild type and one mutant allele of the Kv3.3 gene, we analysed the properties of tetrameric channels formed by mixtures of wild type and mutant subunits. We report that one R420H subunit and at least one R423H subunit can co-assemble with the wild type protein to form active channels. The functional properties of channels containing R420H and wild type subunits strongly resemble those of wild type alone. In contrast, channels containing R423H and wild type subunits show significantly altered gating, including a hyperpolarized shift in the voltage dependence of activation, slower activation, and modestly slower deactivation. Notably, these effects resemble the modified gating seen in channels containing a mixture of F448L and wild type subunits, although the F448L subunit slows deactivation more dramatically than the R423H subunit. Our results suggest that the clinical severity of R423H reflects its dual dominant negative and dominant gain of function effects. However, as shown by R420H, reducing current amplitude without altering gating does not result in infant onset disease. Therefore, our data

N. A. Minassian and M.-C. A. Lin contributed equally to this work.

DOI: 10.1113/jphysiol.2012.228205

strongly suggest that changes in Kv3.3 gating contribute significantly to an early age of onset in SCA13.

(Resubmitted 15 January 2012; accepted 27 January 2012; first published online 30 January 2012)

Corresponding author D. M. Papazian: Department of Physiology, David Geffen School of Medicine at UCLA, Los Angeles, CA 90095-1751, USA. Email: papazian@mednet.ucla.edu

Abbreviations SCA13, spinocerebellar ataxia type 13; τ_{act}, activation time constant; τ_{deact}, deactivation time constant; $V_{1/2}$, activation midpoint voltage.

Introduction

Spinocerebellar ataxia type 13 (SCA13) is a human autosomal dominant disease caused by mutations in the *KCNC3* gene, which encodes the Kv3.3 voltage-gated K^+ channel (Waters *et al.* 2006). Kv3.3 channels have specialized gating properties including a depolarized voltage range for activation, fast activation and very fast deactivation that promote sustained, high-frequency firing of action potentials (Rudy & McBain, 2001). SCA13 mutations alter the functional properties of Kv3.3 channels, raising the possibility that the disease results from changes in the electrical activity of neurons. Recently, we showed that a SCA13 mutation reduces the excitability of Kv3.3-expressing neurons *in vivo* in zebrafish, consistent with the idea that changes in neuronal function initiate pathogenesis in the disease (Issa *et al.* 2011).

SCA13 exists in two forms characterized by onset in infancy or during adulthood. The early-onset form is associated with motor delay, persistent motor deficits and maldevelopment of the cerebellum, whereas the adult-onset form results in progressive cerebellar degeneration accompanied by progressive ataxia (Herman-Bert *et al.* 2000; Waters *et al.* 2006; Figueroa *et al.* 2010, 2011). The age of onset is strongly correlated with the causative mutation in unrelated SCA13 families (Figueroa *et al.* 2010, 2011). However, the relationship between the age of disease onset and the effects of SCA13 mutations on the function of Kv3.3 channels is not well understood. The F448L mutation in the S5 transmembrane segment, which causes early-onset SCA13, results in a robustly active channel protein with significantly altered gating (Waters *et al.* 2006). Two other mutations, R420H and R423H in the S4 segment in the voltage sensor domain, suppress Kv3 current amplitude by a dominant negative mechanism (Waters *et al.* 2006; Figueroa *et al.* 2010). Despite the fact that they both mediate dominant negative suppression, R420H causes adult-onset SCA13 whereas R423H results in early childhood onset (Waters *et al.* 2006; Figueroa *et al.* 2010, 2011).

How the R420H and R423H dominant negative mutations result in distinct clinical forms of SCA13 is unknown. Affected individuals have one wild type and one mutant allele of *KCNC3*. Co-assembly of mutant and wild type subunits is required for dominant negative suppression of channel activity (Schulteis *et al.* 1998). In this study, we tested the hypothesis that a limited number of R420H or R423H subunits can co-assemble with wild type subunits without abolishing channel activity. If this is so, the mutant subunits might have a differential effect on channel function that could contribute to the age of disease onset. To investigate this possibility, we analysed the properties of channels formed by mixed populations of wild type and SCA13 mutant subunits. We found that one R420H subunit and at least one R423H subunit is able to co-assemble with the wild type protein to form active channels. The functional properties of channels formed from a mixture of R420H and wild type subunits strongly resemble those of wild type channels. In contrast, channels containing a mixture of R423H and wild type subunits show significantly altered gating, including a hyperpolarized shift in the voltage dependence of activation, slower activation and moderately slower deactivation. Notably, these effects resemble the changes in gating seen in channels formed from a mixture of wild type and F448L subunits, although F448L slows channel closing more dramatically than R423H. Despite this, R423H and F448L result in similar clinical phenotypes, suggesting that the severity of R423H reflects its dual dominant negative and dominant gain of function effects. However, the R420H mutation clearly indicates that reducing current amplitude without altering gating is insufficient to cause the infant onset form of the disease. Therefore, our results strongly support the idea that altering the specialized gating properties of Kv3.3 channels contributes significantly to an early age of onset in SCA13.

Methods

Ethical approval

Animal procedures were approved by the Chancellor's Animal Research Committee at the University of California at Los Angeles.

Molecular biology

Mutations were introduced into a human wild type Kv3.3 cDNA clone (kind gift of Dr James L. Rae,

Mayo Foundation) using QuikChange (Stratagene) and confirmed by sequencing (Rae & Shepard, 2000). To generate Kv3.3-IR, which lacks N-type inactivation, residues 1–76 were deleted from human Kv3.3 by mutating the first ATG codon. In Kv3.3-IR, translation begins at methionine 77. Similar non-inactivating versions of rat and zebrafish Kv3.3 have been described previously (Desai *et al.* 2008; Mock *et al.* 2010). To prevent K^+ permeation through the central pore, the mutation W495F was introduced into the pore region. W495F in Kv3.3 is equivalent to the non-conducting W434F mutation in Shaker (Perozo *et al.* 1993).

RNA was transcribed *in vitro* using the mMessage mMachine T7 Ultra kit (Ambion). RNA was quantified by absorbance at 260 nm and by agarose gel electrophoresis in comparison to standards of known concentration. *Xenopus laevis* frogs were anaesthetized in 0.1% ethyl 3-aminobenzoate methanesulfonate before harvesting oocytes. RNA was injected into oocytes using standard methods.

Electrophysiology

Wild type and mutant subunits were expressed alone or together by injecting carefully calibrated amounts of RNA. Channel activity was recorded at room temperature 1 to 4 days later using a Warner OC-725C two-electrode voltage clamp (Timpe *et al.* 1988; Papazian *et al.* 1991). Electrodes were filled with 3 M KCl and had resistances of 0.3 to 0.8 MΩ. In most experiments, oocytes were bathed in a solution containing (in mM): 4 KCl, 85 NaCl, 1.8 $CaCl_2$ and 10 Hepes, pH 7.2. As noted, oocytes were bathed in a low pH solution containing (in mM): 4 KCl, 85 NaCl, 1.8 $CaCl_2$ and 10 Mes (2-[*N*-morpholino]ethanesulfonate), pH 5.5. To measure tail currents, the bath solution contained (in mM): 89 RbCl, 2.4 $NaHCO_3$, 0.82 $Ca(NO_3)_2$, 0.41 $CaCl_2$ and 10 Hepes, pH 7.2. Use of 89 mM Rb^+ slows deactivation and increases tail current amplitude, making it easier to quantify the time course of channel closing (Swenson & Armstrong, 1981). To verify that similar results were obtained using the physiologically relevant permeant ion, tail currents were also recorded in the same solution containing 89 mM KCl rather than 89 mM RbCl. It was not feasible to record tail currents in a 4 mM K^+ bath solution because tail current amplitudes were too small.

Known amounts of RNA encoding Kv3.3 wild type, Kv3.3-IR and F448L were separately injected into oocytes to verify that K^+ current amplitude was linearly related to the amount of RNA used. In dominant negative experiments, 1 ng of wild type RNA was mixed with R420H or R423H RNA at ratios indicated in the text. Current amplitudes were measured by pulsing from a holding potential of –90 mV to +40 mV. In each experiment, the amplitudes for wild type controls and wild type/mutant mixtures were measured on the same day, either 2 or 3 days post-injection.

To assess the stoichiometry of dominant negative suppression, experimental results were compared with the predictions of the binomial distribution (Blaine & Ribera, 1998; Manganas & Trimmer, 2000). For each ratio, the relative amounts of wild type and mutant RNA were defined as X and $1-X$, respectively. For example, at a 1:2 ratio, $X = 0.33$ and $1-X = 0.67$. If incorporation of one mutant subunit is sufficient to abolish activity, the fraction of wild type activity remaining at each ratio is predicted to be X^4, corresponding to channels composed of four wild type subunits only. If one mutant subunit is able to incorporate into functional channels, the fraction of wild type activity remaining at each ratio is predicted to be $X^4 + 4 \times X^3 \times (1-X)$, corresponding to the sum of channels composed of four wild type subunits or one mutant plus three wild type subunits. If two mutant subunits are able to incorporate, the fraction of wild type activity remaining at each ratio is predicted to be $X^4 + 4 \times X^3 \times (1-X) + 6 \times X^2 \times (1-X)^2$, corresponding to the sum of channels composed of four wild type subunits or one mutant plus three wild type subunits or two mutant plus two wild type subunits. Applying the binomial distribution assumes that the amount of protein made in oocytes is linearly related to the amount of RNA injected and that mutant and wild type subunits co-assemble randomly (Blaine & Ribera, 1998; Manganas & Trimmer, 2000). As these assumptions can be difficult to verify, we used a second strategy based on inactivation tagging to determine whether mutant subunits can incorporate into active channels, as described in the text.

To characterize the steady-state properties of channel activation, currents were evoked by pulsing from a holding potential of –90 mV to voltages ranging from −40 to +70 mV in 10 mV increments. Assuming a linear open-channel current–voltage relationship, conductance values were calculated from peak current amplitudes using a reversal potential of –80 mV and normalized to the maximum value obtained in the experiment. Normalized conductance values were plotted *versus* test voltage. Data were fitted with a single Boltzmann function to provide values for the midpoint voltage ($V_{1/2}$) and slope factor.

The kinetics of channel opening were characterized by pulsing from a holding potential of –90 mV to voltages ranging from +10 to +70 mV in 10 mV increments except for experiments involving F448L, in which the voltage range was −10 to +70 mV. Current traces were fitted with a single exponential function to estimate the time constant for activation, τ_{act}. The kinetics of channel closing were determined in the 89 mM Rb^+ or 89 mM K^+ bath solutions by pulsing from the holding potential of −90 mV

to +40 mV prior to repolarizing to voltages ranging from −25 to −90 mV in 5 mV increments. Tail currents were fitted with a single exponential function to estimate the time constant for deactivation, τ_{deact}.

To investigate whether the R420H or R423H mutations generated gating pore currents, 16 ng of Kv3.3–W495F, 16–32 ng of R420H–W495F, or 16–32 ng of R423H–W495F RNA was injected alone or 16 ng of Kv3.3–W495F was co-injected with 16 ng of R420H–W495F or 16 ng of R423H–W495F RNA.

Results

R420H subunit can incorporate into active Kv3.3 channels

Kv3.3 channels, like other voltage-gated K^+ channels, are formed by the assembly of four pore-forming subunits (MacKinnon, 1991). In SCA13, affected individuals have one wild type and one mutant allele of *KCNC3* (Waters *et al.* 2006). As a result, mutant and wild type subunits are able to co-assemble, making the properties of channels formed from a mixture of both subunit types particularly relevant to the disease. We compared the functional properties of channels formed by co-expressing wild type subunits with R420H, R423H or F448L mutant subunits to determine whether there is a correlation between changes in channel activity and the age of disease onset in SCA13.

Previously, we showed that R420H and R423H suppress the amplitude of Kv3 currents by a dominant negative mechanism but did not determine whether the incorporation of one mutant subunit into an otherwise wild type tetramer was sufficient to abolish channel activity (Waters *et al.* 2006; Figueroa *et al.* 2010). To investigate the stoichiometry of dominant negative suppression, we injected carefully calibrated amounts of RNA into *Xenopus* oocytes, varying the amount of mutant RNA in the presence of a constant amount (1 ng) of wild type RNA. Current amplitudes were measured 2–3 days later using a two-electrode voltage clamp. Importantly, we verified in control experiments that the average current amplitude was linearly related to the amount of wild type RNA when it was injected alone (data not shown).

R420H subunits are non-functional when expressed alone in oocytes (Waters *et al.* 2006). Co-expression of R420H mutant subunits with wild type Kv3.3 led to a dose-dependent decrease in current amplitude compared with wild type alone (Fig. 1*A*) (Waters *et al.* 2006). We compared the reduction in current amplitude with the predictions of the binomial distribution for three different hypotheses: first, that incorporation of one mutant subunit abolishes channel function; second, that one mutant subunit can be incorporated into active channels; and third, that two mutant subunits can be incorporated into active channels (Fig. 1*B*). Use of the binomial distribution assumes that the amount of protein made in oocytes is linearly related to the amount of RNA injected, and that mutant and wild type subunits co-assemble randomly (Blaine & Ribera, 1998; Manganas & Trimmer, 2000).

Wild type and R420H subunits were expressed at ratios ranging from 1:0.25 to 1:4 (WT:R420H). Residual current amplitudes, shown as per cent of wild type activity, agreed well with that predicted if one mutant subunit is able to incorporate into functional channels. In contrast, the remaining current amplitudes were greater than predicted if one mutant subunit were sufficient to abolish activity and less than predicted if two mutant subunits were able to incorporate into active channels (Fig. 1*B*).

One caveat in this experiment is that non-functional mutant proteins such as R420H may turn over more rapidly than the wild type protein (Myers *et al.* 2004). If so, the predictions of the binomial distribution would not be applicable because the amount of mutant protein would be less than expected relative to the amount of RNA injected. This would inflate the residual current amplitude because the fraction of channels comprising wild type subunits only would be greater than predicted.

We therefore used an alternative strategy based on inactivation tagging to verify that R420H subunits are able to incorporate into functional channels (MacKinnon *et al.* 1993; Tiwari-Woodruff *et al.* 1997; Schulteis *et al.* 1998). The Kv3.3 protein contains an N-terminal extension that mediates N-type inactivation by blocking the internal mouth of the pore (Desai *et al.* 2008). Deleting the N-terminal extension eliminates N-type inactivation (Desai *et al.* 2008; Mock *et al.* 2010). However, incorporation of a single subunit containing the N-terminal extension is sufficient to confer inactivation on the channel, although it occurs at a slower rate than in channels composed of four inactivating subunits (MacKinnon *et al.* 1993).

We generated a non-inactivating form of Kv3.3, Kv3.3-IR (inactivation removed), by deleting the N-terminal extension and then co-expressed it with R420H in the normal, inactivating background at ratios of 1:1 and 1:4 (IR:R420H) (Fig. 1*C*) (Desai *et al.* 2008). For comparison, wild type Kv3.3 and Kv3.3-IR channels were expressed separately. Currents were evoked by pulsing from −80 to +40 mV. Traces were scaled to the same amplitude and overlaid. Inactivating components of current were evident at both expression ratios. These data indicate that R420H subunits have incorporated into active channels because only the mutant subunit can confer inactivation. Increasing the ratio from 1:1 to 1:4 resulted in faster inactivation, although at the 1:4 ratio channels inactivated more slowly than wild type Kv3.3, as expected if the number of inactivating mutant

subunits that can integrate into active channels is limited (MacKinnon *et al.* 1993). These results confirm that R420H subunits are able to incorporate into functional channels.

To estimate the extent of inactivation, we divided the current amplitude at the end of a 500 ms pulse by the peak amplitude (Fig. 1*D*). The value of I_{500ms}/I_{peak} averaged 0.63 ± 0.03 at a 1:1 ratio and 0.13 ± 0.03 at 1:4, compared with 0.03 ± 0.005 for wild type Kv3.3 and 0.92 ± 0.004 for Kv3.3-IR. It is worth noting that I_{500ms}/I_{peak} for Kv3.3-IR was less than 1 due to the presence of C-type inactivation (Hoshi *et al.* 1991; Baukrowitz & Yellen, 1995). As inactivation was slow and current amplitudes were small at the 1:1 and 1:4 ratios, we did not fit the time course of inactivation to estimate a time constant (τ_{inact}).

Incorporation of R420H subunit into active Kv3.3 channels has little effect on function

We next investigated whether incorporation of R420H subunits alters the functional properties of Kv3.3 channels. Wild type and R420H subunits were co-expressed at ratios of 1:1, 1:2 and 1:4 (WT:R420H). In these experiments, both types of subunit contained the N-terminal extension that mediates N-type inactivation. To characterize the steady-state properties of channel activation, currents were evoked by pulsing to voltages ranging from −40 to +70 mV. Peak current amplitudes were converted to normalized conductance values, which were plotted as a function of voltage (Fig. 2*A*). Data sets were fitted with single Boltzmann functions to obtain values for the mid-point voltage ($V_{1/2}$) and slope factor. At a 1:1 ratio of

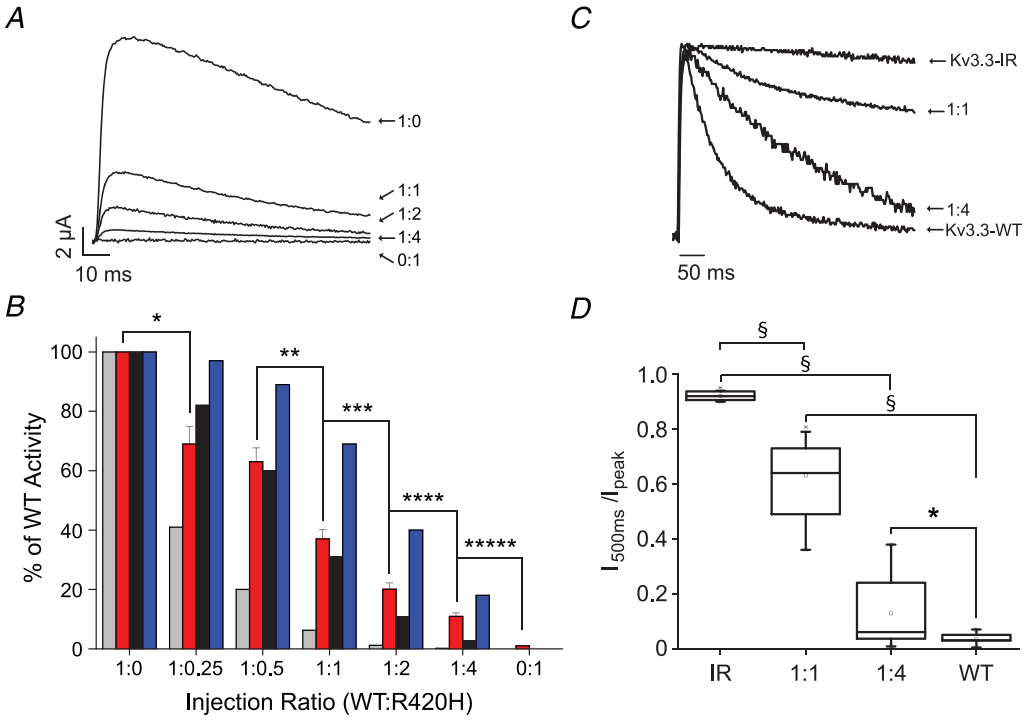

Figure 1. One R420H subunit can incorporate into functional Kv3.3 channels
A, RNA encoding wild type and R420H subunits was injected into oocytes at the indicated ratios (WT:R420H). Currents were evoked by pulsing from −90 mV to +40 mV. Representative examples are shown. *B*, bar graph shows normalized peak current amplitudes measured at +40 mV for the indicated ratios of wild type and R420H RNA (2nd bar from left at each ratio). Values are provided as mean ± SEM, $n = 19$–45. Significance was tested using a one-way ANOVA followed by 2 sample *t* test, $P < 0.05$: *different from 1:0; **different from 1:0.5; ***different from 1:1; ****different from 1:2; *****different from 1:4. Also shown are the predictions of the binomial distribution for the hypotheses that one mutant subunit abolishes activity (1st bar) or that one (3rd bar) or two (4th bar) mutant subunits can incorporate into functional channels. The graph differs somewhat from published data because the amount of wild type RNA used in previous experiments was sometimes beyond the linear response range (Waters *et al.* 2006). *C*, Kv3.3-IR and R420H subunits were expressed at the indicated ratios (IR:R420H) or Kv3.3-IR and wild type were expressed alone. Current traces were evoked by pulsing from −80 mV to +40 mV. Representative examples, scaled to the same amplitude and overlaid, are shown. *D*, box plot shows normalized I_{500ms}/I_{peak} values measured at +40 mV for the indicated ratios of Kv3.3-IR and R420H subunits. For comparison, values obtained with Kv3.3-IR or wild type expressed alone are also shown. Indicated pairs differed significantly by one-way ANOVA followed by 2 sample *t* test: §$P < 0.00001$; *$P < 0.05$ (Kv3.3-IR, $n = 21$; 1:1, $n = 18$; 1:4, $n = 13$; wild type, $n = 15$).

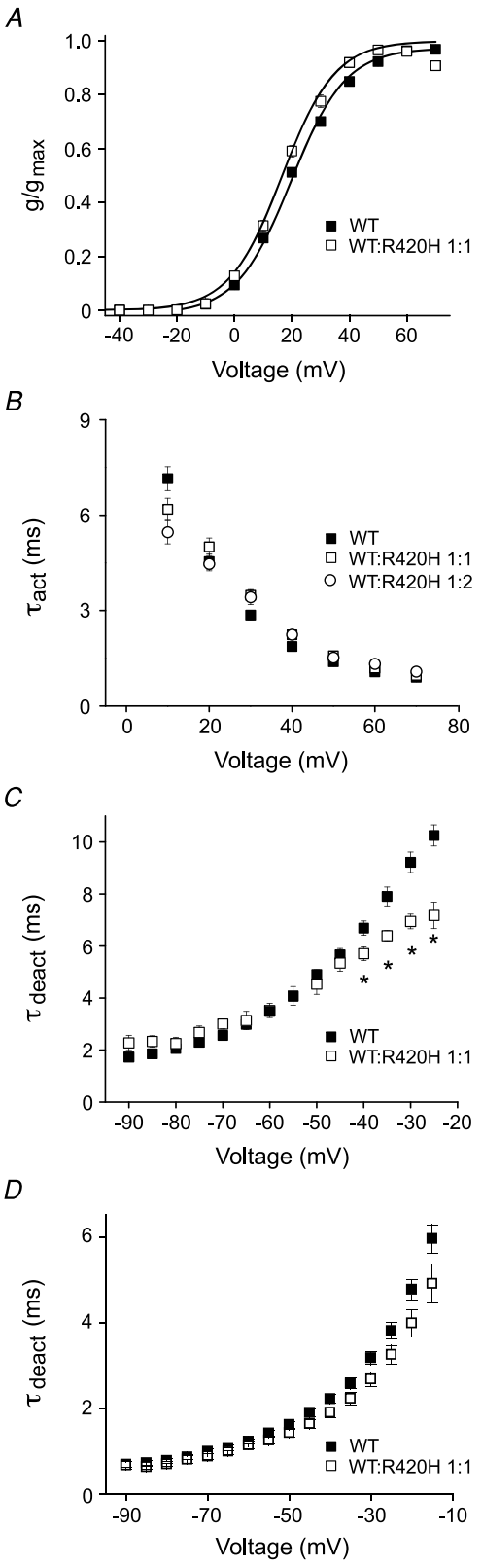

Figure 2. R420H subunits have little effect on the functional properties of Kv3.3 channels
A, normalized conductance has been plotted as a function of voltage for wild type Kv3.3 expressed alone (■, $n = 155$) or with R420H at a 1:1 ratio (□, $n = 29$). Values are provided as mean ± SEM. Here and in subsequent figures, if error bars are not visible they are smaller than the size of the symbol. Data sets were fitted with single Boltzmann functions (continuous lines). Midpoint voltages and slope factors are shown in Table 1. Results obtained at ratios of 1:2 and 1:4 did not differ significantly from 1:1 (data not shown). *B*, currents were evoked by pulsing from –90 mV to voltages ranging from +10 to +70 mV in 10 mV increments. Current traces were fitted with a single exponential function to estimate the time constant for activation (τ_{act}), which has been plotted *versus* voltage. Data are shown for wild type expressed alone (■, $n = 48$) or co-injected with R420H at ratios of 1:1 (□, $n = 9$) and 1:2 (o, $n = 9$). Values are provided as mean ± SEM. Values of τ_{act} did not differ significantly (one-way ANOVA followed by 2 sample *t* test, $P \geq 0.05$). *C*, tail currents were recorded in a high Rb^+ bath solution by repolarizing from +40 mV to voltages ranging from −25 to –90 mV in 5 mV increments. Traces were fitted with a single exponential function to estimate the time constant for deactivation (τ_{deact}), which has been plotted *versus* repolarization voltage. Data are shown for wild type expressed alone (■, $n = 36$) or with R420H at a 1:1 ratio (□, $n = 11$). Values are provided as mean ± SEM. Between –25 and –40 mV, values of τ_{deact} differed significantly by ANOVA followed by 2 sample *t* test (*$P < 0.05$). At ratios of 1:2 and 1:4, tail currents were too small to measure. *D*, tail currents were recorded in a high K^+ bath solution by repolarizing from +40 mV to voltages ranging from −15 to −90 mV in 5 mV increments. Traces were fitted with a single exponential function to estimate τ_{deact}, which has been plotted *versus* repolarization voltage. Data are shown for wild type expressed alone (■, $n = 9$) or with R420H at a 1:1 ratio (□, $n = 11$). Values are provided as mean ± SEM. Values of τ_{deact} did not differ significantly by ANOVA followed by 2 sample *t* test ($P \geq 0.05$).

wild type and R420H subunits, $V_{1/2}$ was slightly shifted by –3 mV with no change in the slope factor (Fig. 2*A*, Table 1). Similar results were obtained at the 1:2 and 1:4 ratios (data not shown).

We also characterized opening and closing kinetics in channels formed from a mixture of wild type and R420H subunits. Currents were evoked by depolarizing to voltages ranging from +10 to +70 mV. Current traces were fitted with a single exponential function to estimate the time constant of activation (τ_{act}), which was plotted *versus* test potential (Fig. 2*B*). No significant differences were detected in the presence and absence of R420H subunits (Fig. 2*B*, Table 1). To obtain values for the time constant of deactivation (τ_{deact}), wild type and R420H subunits were expressed at a 1:1 ratio. Currents were recorded in bath solutions containing 89 mM Rb^+ or 89 mM K^+ by pulsing from –90 to +40 mV prior to repolarizing to tail potentials ranging from −25 to –90 mV (Rb^+) or –15 to –90 mV (K^+). Tail currents were fitted with single exponential functions and values of τ_{deact} were plotted *versus* repolarization voltage (Fig. 2*C* and *D*). In the presence of R420H subunits, small but statistically significant increases in the rate of deactivation were detected in the Rb^+ bath solution at tail voltages ranging from –40 to –25 mV (Fig. 2*C*, Table 1). Although a similar trend was observed in the K^+ bath solution, the differences were not

Table 1. Steady state and kinetic parameters of Kv3.3 channels containing SCA13 mutant subunits

	$V_{1/2}$ (mV)	Slope (mV)	τ_{act} +20 mV (ms)	τ_{deact} −40 mV (ms)*	τ_{deact} −60 mV (ms)*
Wild type	19.5 ± 0.3	9.4 ± 0.2	4.7 ± 0.2	6.3 ± 0.2	3.3 ± 0.1
R420H	NA	NA	NA	NA	NA
WT: R420H 1:1	16.6 ± 0.6	9.2 ± 0.5	5.0 ± 0.3	5.7 ± 0.3	3.5 ± 0.3
R423H	3.0 ± 0.8†	11.1 ± 2.9†	10.0 ± 1.9†	ND	ND
WT: R423H 1:1	10.1 ± 0.6‡	9.4 ± 0.5‡	9.7 ± 1.2‡	9.7 ± 0.5	4.7 ± 0.2
F448L	3.3 ± 0.4†	9.7 ± 0.3†	8.0 ± 0.4†	85.7 ± 2.7	41.7 ± 1.9
WT: F448L 1:1	10.8 ± 0.5‡	10.0 ± 0.3‡	7.9 ± 0.5‡	51.4 ± 3.5	23.5 ± 1.6

NA, not applicable; ND, not done. *Measured in 89 mm RbCl bath solution; †no significant difference between values for R423H and F448L expressed alone; ‡no significant difference between values for WT:R423H at a 1:1 ratio and WT:F448L at a 1:1 ratio.

statistically significant (Fig. 2*D*). The results obtained in the Rb^+ bath solution reinforce the conclusion that R420H subunits are able to incorporate into active channels. However, in the presence of the physiologically relevant permeant ion, K^+, the mutant subunit has little effect on the functional properties of the channel. Our data indicate that R420H suppresses Kv3.3 current amplitude but the functional characteristics of the residual K^+ current are similar to those of wild type.

Voltage-dependent transport of protons has not been detected in R420H

We also investigated whether the R420H mutation renders the Kv3.3 voltage sensor leaky to protons. Mutations in the voltage-gated Na^+ channel Nav1.4 cause hypokalaemic periodic paralysis (Cannon, 2010; Catterall, 2010). Mutations at the first or second arginine residue in the S4 segment of domain II generate pathological gating pore currents, which flow through the voltage sensor domain rather than the central, Na^+-selective pore (Sokolov *et al.* 2007; Struyk & Cannon, 2007). A mutation that converts the first arginine in the domain II S4 to histidine generates proton-selective gating pore currents activated by hyperpolarization (Struyk & Cannon, 2007). The SCA13 mutation R420H changes the third arginine in the Kv3.3 S4 segment to histidine. In Shaker, the analogous mutation, R368H, results in voltage-dependent H^+ transport through the voltage sensor domain in the presence of a pH gradient (Starace *et al.* 1997; Starace & Bezanilla, 2001). Transport activity exhibits a bell-shaped dependence on voltage, with maximal activity in the voltage range corresponding to the most frequent voltage sensor conformational changes.

To better detect small currents through the voltage sensor domain, the W495F mutation was introduced into the wild type and R420H mutant subunits. In Shaker, the analogous mutation, W434F, is non-conducting (Perozo *et al.* 1993). Similarly, the W495F mutation in Kv3.3 abolished ionic conductance through the central pore (Fig. 3*A*).

To determine whether the incorporation of R420H subunits results in ion transport through the voltage sensor domain, WT–W495F and R420H–W495F subunits were co-expressed at a 1:1 ratio. Voltage clamp experiments were conducted in neutral (pH 7.2) or acidic (pH 5.5) bath solutions. Currents were evoked by pulsing from a holding potential of −90 mV to voltages ranging from −90 to +60 mV in 10 mV increments and recorded without leak subtraction. Only linear leak currents were detected (Fig. 3*B*). Comparable results were obtained when the R420H–W495F subunit was expressed alone (data not shown). Similar linear leak currents were observed when the WT–W495F subunit was expressed alone and in uninjected and mock-injected oocytes (Fig. 3*A*, *C* and *D*).

R423H mutant subunits incorporate into functional channels

Similarly to R420H, the R423H subunit reduces Kv3 current amplitude by a dominant negative mechanism (Fig. 4*A*) (Figueroa *et al.* 2010). We investigated the stoichiometry of this effect by co-expressing wild type and mutant subunits at ratios ranging from 1:0.25 to 1:4 (WT:R423H) (Fig. 4*B*). The results were compared with the predictions of the binomial distribution. Residual current amplitudes were incompatible with the idea that one mutant subunit is sufficient to abolish activity. At ratios of 1:0.25, 1:0.5 and 1:1 (WT:R423H), the fraction of remaining activity agreed well with that predicted if one mutant subunit can incorporate into functional channels. However, at ratios of 1:2 and 1:4, current amplitudes were significantly greater than expected if only one mutant subunit were present in active channels. Instead, amplitudes were similar to that expected if two mutant subunits were able to assemble into active channels. These results suggest that more than one mutant subunit can be incorporated when expressed in excess over the wild type subunit.

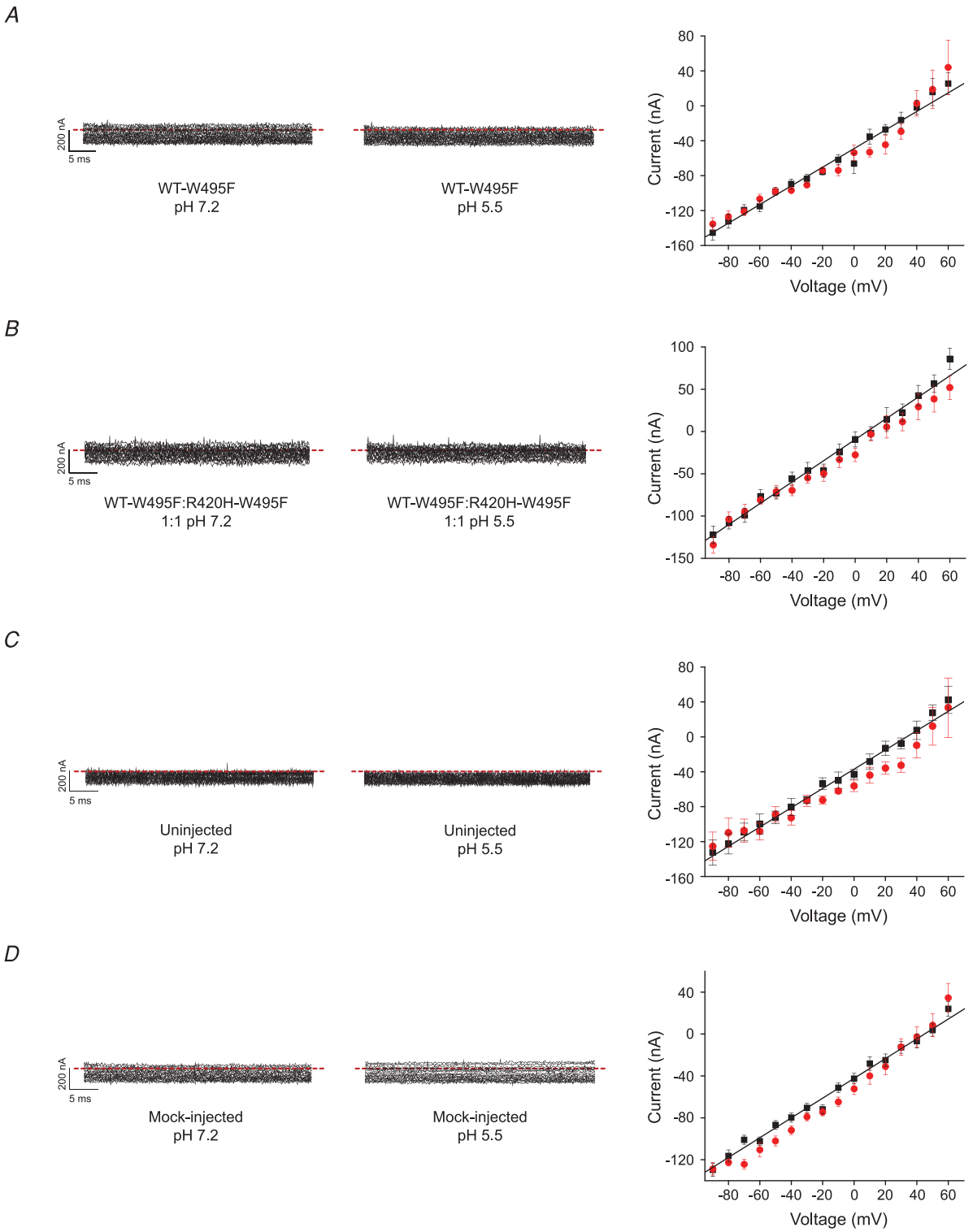

Figure 3. R420H mutation does not generate detectable gating pore currents in oocytes
Data are shown for: *A*, WT:W495F expressed alone; *B*, WT:W495F and R420H:W495F expressed at a 1:1 ratio; *C*, uninjected oocytes; and *D*, oocytes injected with RNase-free water (mock-injected). Each panel shows representative, unsubtracted current traces recorded at pH 7.2 (left) or 5.5 (centre) by pulsing from –90 mV to voltages ranging from −90 to +60 mV in 10 mV increments. Dashed lines indicate the 0 current level. Right: current amplitudes measured at pH 7.2 (squares) or 5.5 (circles) have been plotted *versus* voltage. Values are provided as mean ± SEM. The continuous line shows a linear regression fit to the pH 7.2 data.

To verify that R423H subunits incorporate into functional channels, we used the inactivation tagging strategy (MacKinnon *et al.* 1993; Tiwari-Woodruff *et al.* 1997; Schulteis *et al.* 1998). Kv3.3-IR subunits were co-expressed with R423H subunits at ratios of 1:1 and 1:4 (IR:R423H) (Fig. 4*C*). For comparison, wild type Kv3.3 and Kv3.3-IR channels were expressed separately. Currents were recorded by pulsing from –80 to +40 mV. Traces were scaled to the same amplitude and overlaid. Substantial inactivating components were detected at ratios of 1:1 and 1:4 (WT:R423H) (Fig. 4*C* and *D*). At the 1:4 ratio, the rate and extent of inactivation were similar to that of wild type channels (Fig. 4*C*). This was confirmed by measuring the extent of inactivation, expressed as

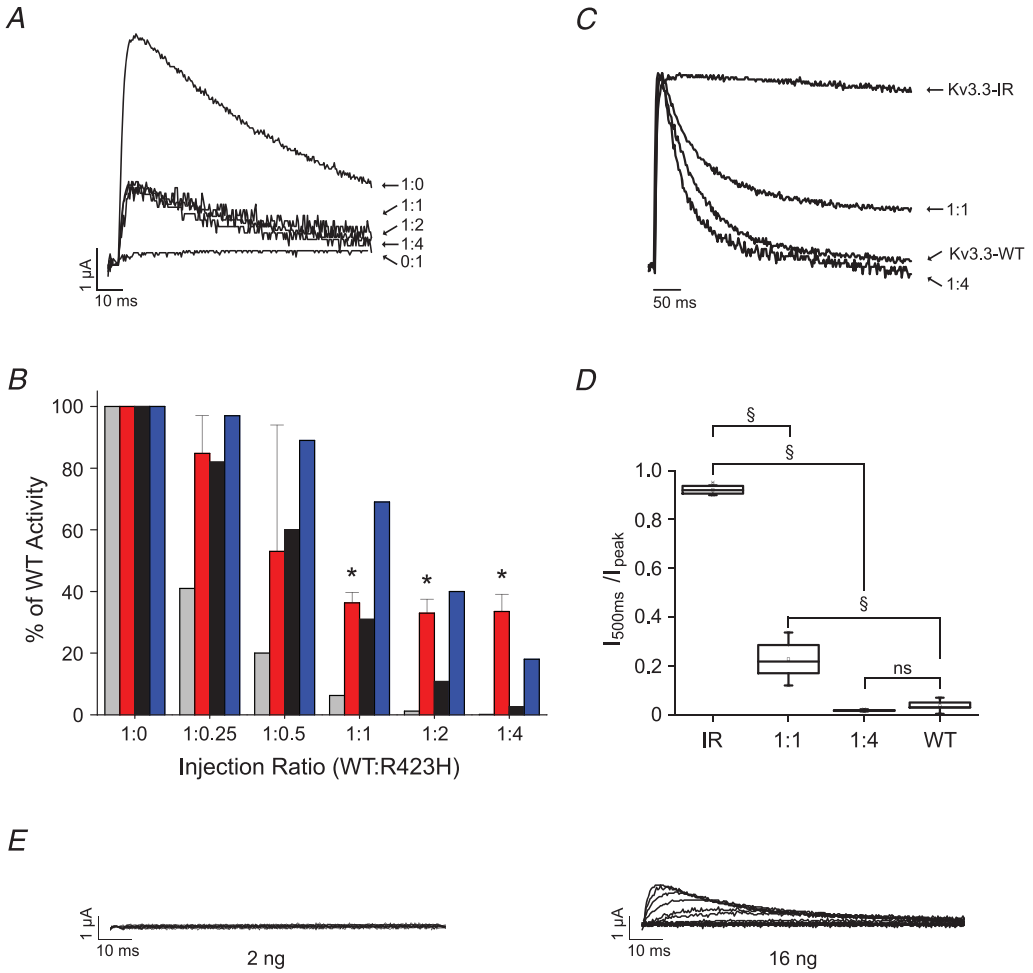

Figure 4. At least one R423H subunit can incorporate into functional Kv3.3 channels
A, RNA encoding wild type and R423H subunits was injected into oocytes at the indicated ratios (WT:R423H). Currents were evoked by pulsing from −90 mV to +40 mV. Representative examples are shown. *B*, bar graph shows normalized peak current amplitudes measured at +40 mV for the indicated ratios of wild type and R423H (2nd bar from left at each ratio). Values are provided as mean ± SEM, $n = 3$–32. Indicated values differed significantly from wild type expressed alone by one-way ANOVA followed by 2 sample *t* test (*$P < 0.05$). Also shown are the predictions of the binomial distribution for the hypotheses that one mutant subunit abolishes activity (1st bar) or that one (3rd bar) or two (4th bar) mutant subunits can incorporate into functional channels. The graph differs somewhat from published data because the amount of wild type RNA used in previous experiments was sometimes beyond the linear response range (Figueroa *et al.* 2010). *C*, Kv3.3-IR and R423H subunits were expressed at the indicated ratios (IR:R423H) or Kv3.3-IR and wild type were expressed alone. Current traces were evoked by pulsing from −80 mV to +40 mV. Representative examples, scaled to the same amplitude and overlaid, are shown. *D*, box plot shows normalized I_{500ms}/I_{peak} values measured at +40 mV for the indicated ratios of Kv3.3-IR and R423H subunits. For comparison, values obtained with Kv3.3-IR or wild type expressed alone are also shown. Indicated pairs differed significantly by one-way ANOVA followed by 2 sample *t* test: §$P < 0.00001$; ns, not significant (Kv3.3-IR, $n = 21$; 1:1, $n = 10$; 1:4, $n = 5$; wild type, $n = 15$). *E*, RNA encoding R423H (2 ng or 16 ng, as indicated) was injected into oocytes. Traces were recorded by stepping from –90 mV to voltages ranging from −80 to +70 mV in 10 mV increments. Representative results are shown.

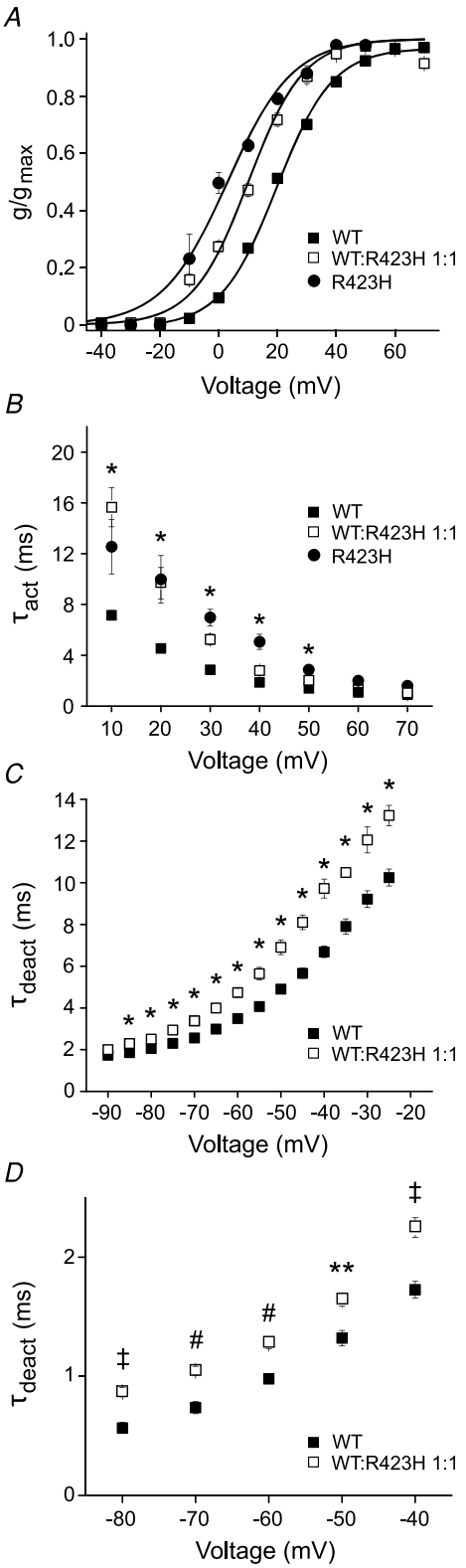

Figure 5. R423H subunits affect the specialized gating properties of Kv3.3 channels
A, normalized conductance has been plotted as a function of voltage for wild type Kv3.3 (■, $n = 155$) or R423H (● , $n = 4$) expressed alone or for wild type and R423H expressed at a 1:1 ratio (□, $n = 35$). Values are provided as mean ± SEM. Data sets were fitted with single Boltzmann functions (continuous lines). Midpoint voltages and slope factors are shown in Table 1. *B*, current traces were fitted with a single exponential function to estimate τ_{act}, which has been plotted *versus* voltage. Data are shown for wild type (■, $n = 48$) or R423H (● , $n = 4$) expressed alone and for wild type and R423H expressed at a 1:1 ratio (□, $n = 7$). Values are provided as mean ± SEM. As indicated, R423H expressed alone or in a 1:1 ratio with wild type differed significantly from wild type expressed alone by one-way ANOVA followed by 2 sample *t* test (*$P < 0.05$). *C*, tail currents were recorded in a high Rb^+ bath solution by repolarizing from +40 mV to voltages ranging from −25 to –90 mV. Traces were fitted with a single exponential function to estimate τ_{deact}, which has been plotted *versus* repolarization voltage. Data are shown for wild type expressed alone (■, $n = 36$) or with R423H at a 1:1 ratio (□, $n = 4$). Values are provided as mean ± SEM. Values of τ_{deact} differed significantly by ANOVA followed by 2 sample *t* test (*$P < 0.05$). When R423H was expressed alone, tail currents were too small to measure. *D*, tail currents were recorded in a high K^+ bath solution by repolarizing from +40 mV to voltages ranging from −40 to –80 mV in 10 mV increments. Traces were fitted with a single exponential function to estimate τ_{deact}, which has been plotted *versus* repolarization voltage. Data are shown for wild type expressed alone (■, $n = 8$–11) or with R423H at a 1:1 ratio (□, $n = 19$). Values are provided as mean ± SEM. Values of τ_{deact} differed significantly by ANOVA followed by 2 sample *t* test (#$P < 0.0001$; ‡$P < 0.0005$; **$P < 0.001$).

I_{500ms}/I_{peak} (Fig. 4*D*). At a 1:1 ratio, the value of I_{500ms}/I_{peak} was 0.23 ± 0.07 compared with 0.92 ± 0.004 for Kv3.3-IR or 0.03 ± 0.005 for wild type expressed alone. In contrast, at a 1:4 expression ratio, the value of I_{500ms}/I_{peak} was 0.02 ± 0.003, which does not differ significantly from wild type expressed alone.

As the rate of N-type inactivation depends on the number of inactivating subunits, our results at the 1:4 ratio suggest that active channels containing predominantly R423H subunits are generated when mutant RNA is injected in substantial excess over wild type (MacKinnon *et al.* 1993; Tiwari-Woodruff *et al.* 1997; Schulteis *et al.* 1998). This finding, in conjunction with the unexpectedly large current amplitudes measured after co-injecting wild type and mutant RNA at ratios of 1:2 and 1:4, raises the possibility that R423H subunits, when expressed in large quantities, may be able to form functional channels in the absence of wild type subunits. Indeed, although injecting 2 ng of R423H RNA did not result in detectable currents in oocytes, injecting 16 ng of R423H RNA generated currents averaging 1.3 ± 0.1 μA at +60 mV (Fig. 4*E*). By comparison, injecting 1 ng of wild type Kv3.3 RNA resulted in currents averaging 12.6 ± 1.3 μA at +60 mV. These results indicate that R423H subunits are able to form functional channels on their own, but do so very inefficiently compared with wild type.

R423H subunits alter Kv3.3 gating

Wild type and R423H subunits were co-expressed to investigate whether the incorporation of mutant subunits alters the functional properties of Kv3.3 channels. In addition, R423H subunits were expressed alone by injecting 16 ng of RNA to detect the activity of R423H homotetramers. To characterize the steady-state properties of channel activation, peak current amplitudes were measured, converted to normalized conductance values, and plotted as a function of voltage (Fig. 5*A*). Data sets were fitted with single Boltzmann functions to obtain values for the midpoint voltage ($V_{1/2}$) and slope factor (Table 1). In R423H homotetramers, $V_{1/2}$ was shifted ~16 mV in the hyperpolarized direction compared with wild type Kv3.3 (Fig. 5*A*, Table 1). In channels formed from a 1:1 ratio of wild type and R423H subunits, $V_{1/2}$ was 10.1 ± 0.6 mV, a value intermediate to channels formed exclusively from wild type (19.5 ± 0.3 mV) or R423H (3.0 ± 0.8 mV) subunits. The slope factor was not significantly altered (Table 1).

To investigate the effect of R423H subunits on activation kinetics, current traces were fitted with single exponential functions to obtain values for τ_{act}, which were plotted *versus* test potential (Fig. 5*B*, Table 1). Compared with wild type, activation was slowed significantly between +10 and +50 mV when the R423H subunit was expressed alone or at a 1:1 ratio with wild type. Activation kinetics were similar in channels containing only R423H subunits or a mixture of wild type and mutant subunits. The R423H subunit had no significant effect on τ_{act} at +60 and +70 mV where channels open at the maximal rate.

To determine whether the R423H mutation alters the kinetics of channel closing, tail currents were recorded in bath solutions containing 89 mM Rb^+ or 89 mM K^+. Traces were fitted with single exponential functions and values of τ_{deact} were plotted *versus* repolarization voltage. In the Rb^+ bath solution, channels formed from a mixture of R423H and wild type subunits deactivated significantly more slowly than wild type channels between −85 and –25 mV (Fig. 5*C*, Table 1). In the K^+ bath solution, deactivation was also significantly slowed in the presence of R423H subunits although the effect was modest (Fig. 5*D*). It was not feasible to determine τ_{deact} for channels composed exclusively of R423H subunits because tail current amplitudes were too small.

In addition to dominant negative suppression of Kv3 current amplitude, our results indicate that the R423H mutant subunit significantly alters channel gating when expressed alone or in combination with wild type Kv3.3. The gating properties of Kv3 channels that facilitate high-frequency spiking in neurons, including the depolarized activation range, fast activation and very fast deactivation, are specifically affected by the R423H mutation.

Voltage-dependent proton permeability has not been detected in R423H

R423H mutates the fourth arginine in the Kv3.3 S4 segment to histidine. In Shaker, the analogous mutation, R371H, converts the voltage sensor domain into a voltage-dependent H^+ transporter as well as a depolarization-activated, H^+-permeable pore (Starace & Bezanilla, 2001). To determine whether the incorporation of R423H subunits into Kv3.3 channels results in H^+ permeability through the voltage sensor domain, WT–W495F and R423H–W495F subunits were co-expressed at a 1:1 ratio for voltage clamp analysis at pH 5.5 and 7.2. Currents were evoked by pulsing from a holding potential of –90 mV to voltages ranging

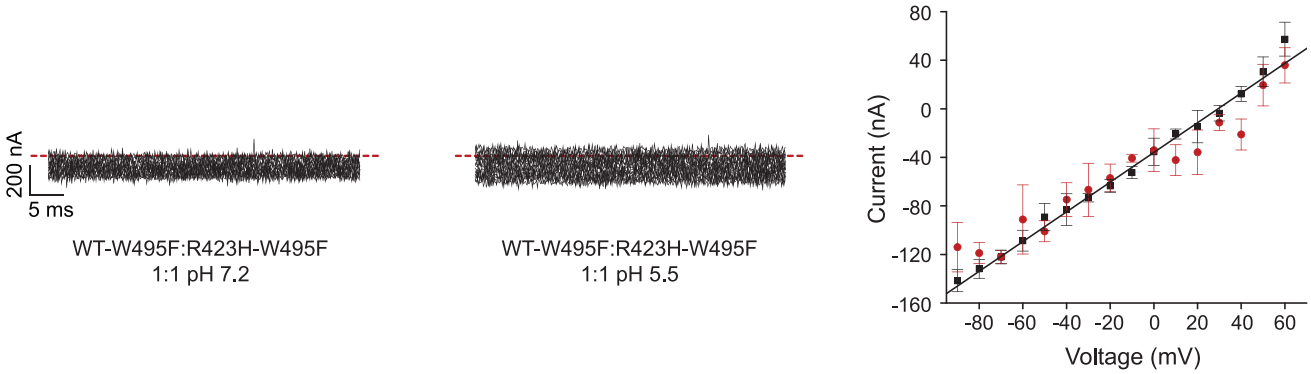

Figure 6. R423H mutation does not generate detectable gating pore currents in oocytes
WT-W495F and R423H-W495H subunits were expressed at a 1:1 ratio. Shown are representative, unsubtracted current traces recorded at pH 7.2 (left) or 5.5 (centre) by pulsing from –90 mV to voltages ranging from −90 to +60 mV in 10 mV increments. Dashed lines indicate the 0 current level. Right: current amplitudes measured at pH 7.2 (squares) or 5.5 (circles) have been plotted *versus* voltage. Values are provided as mean ± SEM. The continuous line shows a linear regression fit to the pH 7.2 data.

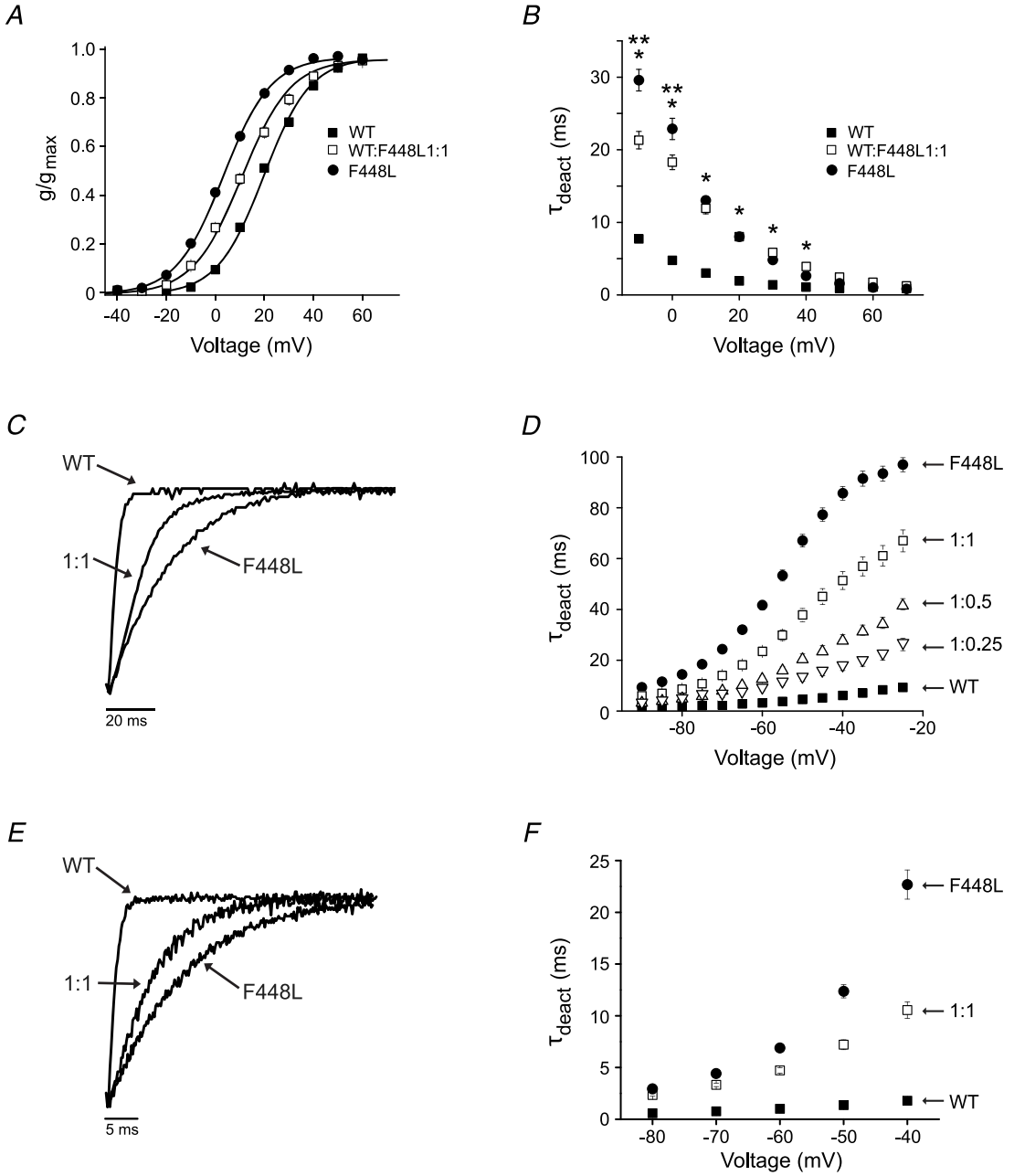

Figure 7. F448L and R423H subunits have similar effects on Kv3.3 channel gating
A, normalized conductance has been plotted as a function of voltage for wild type Kv3.3 (■, $n = 218$) or F448L (● , $n = 74$) expressed alone and for wild type and F448L expressed at a 1:1 ratio (□, $n = 49$). Values are provided as mean ± SEM. Data sets were fitted with single Boltzmann functions (continuous lines). Midpoint voltages and slope factors are shown in Table 1. *B*, current traces were fitted with a single exponential function to estimate τ_{act}, which has been plotted *versus* voltage. Data are shown for wild type (■) or F448L (●) expressed alone and for wild type and F448L expressed at a 1:1 ratio (□). Values are provided as mean ± SEM ($n \geq 25$) and differed significantly by one-way ANOVA followed by 2 sample *t* test, $P < 0.05$ (*F448L alone and 1:1 ratio differ from wild type; **1:1 differs from F448L alone). *C*, tail currents were recorded in a high Rb^+ bath solution by pulsing from −90 to +40 mV prior to repolarizing to –65 mV for wild type or F448L expressed alone or for wild type expressed at a 1:1 ratio with F448L as indicated. Representative results are shown. *D*, tail currents were evoked in high Rb^+ by repolarizing from +40 mV to voltages ranging from −25 to –90 mV. Tail current traces were fitted with a single exponential function to estimate τ_{deact}, which has been plotted *versus* repolarization voltage for wild type (■) or F448L (●) expressed alone and for wild type and F448L expressed at ratios of 1:0.25 (▽), 1:0.5 (△) and 1:1 (□). Values are provided as mean ± SEM, $n \geq 25$. All τ_{deact} values differed significantly from wild type expressed alone, $P < 0.05$ by Student's *t* test, except for the 1:0.25 ratio measured at –90 mV. *E*, tail currents were

from −90 to +60 mV in 10 mV increments and recorded without leak subtraction. Only linear leak currents were detected (Fig. 6). Similar results were obtained when the R423H–W495F subunit was expressed alone (data not shown).

F448L and R423H mutations have similar effects on channel gating

In contrast to R420H and R423H, the F448L protein is robustly active when expressed alone in oocytes. Previously, we showed that the F448L mutation shifts the voltage dependence of activation in the hyperpolarized direction and dramatically slows channel closing (Waters *et al.* 2006). To characterize the functional properties of channels formed by mixtures of wild type and F448L mutant subunits, RNA was injected at a 1:1 ratio. For comparison, WT and F448L subunits were also expressed alone. Channels formed by a 1:1 ratio of wild type and mutant subunits activated over an intermediate voltage range compared with wild type or F448L homotetrameric channels (Fig. 7*A*). At a ratio of 1:1, $V_{1/2}$ was 10.8 ± 0.5 mV, a value that differed significantly compared with either wild type or F448L channels, which were 19.5 ± 0.3 mV and 3.3 ± 0.4 mV, respectively (Table 1). The slope factor was unaffected. Interestingly, there was no significant difference between $V_{1/2}$ values of channels formed from a 1:1 mixture of wild type and F448L RNA or wild type and R423H RNA (Table 1).

Between −10 and +40 mV, channels formed from F448L subunits alone or by co-expression of wild type and F448L subunits activated significantly more slowly than wild type channels (Fig. 7*B*, Table 1). At −10 and 0 mV, values of τ_{act} measured after expressing F448L alone or at a 1:1 ratio with wild type differed significantly. Interestingly, the F448L and R423H mutations had strikingly similar effects on τ_{act} in homotetrameric channels and after expression with wild type at a 1:1 ratio (Table 1). Similarly to R423H, F448L subunits did not significantly alter the minimum value of τ_{act} obtained at very depolarized voltages, consistent with our previous observation that the time course of opening at +60 mV is similar in wild type and F448L channels (Waters *et al.* 2006).

Previously, we showed that channels formed exclusively by F448L subunits deactivated significantly more slowly than wild type in 89 mM Rb^+ (Waters *et al.* 2006). To characterize the effect of F448L on deactivation kinetics in channels formed by a mixture of mutant and wild type subunits, tail currents were recorded in bath solutions containing 89 mM Rb^+ or 89 mM K^+. Traces were fitted with single exponential functions and values of τ_{deact} were plotted *versus* repolarization voltage (Fig. 7*C*–*F*). Channels formed by mixtures of wild type and F448L subunits closed with intermediate kinetics in 89 mM Rb^+ (Fig. 7*C* and *D*, Table 1). Mutant subunits exerted a graded effect on the rate of channel closing, with dose-dependent increases in τ_{deact} (Fig. 7*D*). At –40 mV, τ_{deact} was approximately 8.5-fold greater at a 1:1 ratio of wild type and F448L subunits compared with wild type expressed alone. F448L also slowed channel closing in 89 mM K^+ (Fig. 7*E* and *F*). At –40 mV, τ_{deact} was approximately 5-fold greater at a 1:1 ratio of wild type and F448L subunits compared with wild type expressed alone (Fig. 7*F*). F448L subunits slowed channel closing more dramatically than R423H subunits (Table 1).

Discussion

The available clinical information suggests that the phenotypes of individuals with the R423H and F448L mutations overlap significantly (Herman-Bert *et al.* 2000; Waters *et al.* 2006; Figueroa *et al.* 2010, 2011). Similarities include an early age of disease onset, motor delay, persistent motor deficits and abnormalities in cerebellar structure detected during childhood. Cognitive impairment and seizures have also been reported. This picture contrasts sharply with the phenotype of individuals with the R420H mutation, who experience progressive ataxia and progressive cerebellar degeneration starting in the third decade of life or later (Waters *et al.* 2006; Figueroa *et al.* 2010, 2011). These distinct forms of SCA13 recur in unrelated families, indicating that the clinical features depend on the causative mutation rather than differences in genetic background (Figueroa *et al.* 2010, 2011).

Our previous studies did not clarify the relationship between these distinct clinical phenotypes and the effects of SCA13 mutations on Kv3.3 channel function. We showed that the F448L mutation alters gating, shifting

recorded in a high K^+ bath solution by pulsing from −90 to +40 mV prior to repolarizing to –50 mV for wild type or F448L expressed alone or for wild type expressed at a 1:1 ratio with F448L as indicated. Note change in scale compared to panel *C*. Representative results are shown. *F*, tail currents were evoked in high K^+ by repolarizing from +40 mV to voltages ranging from −40 to –80 mV in 10 mV increments. Tail current traces were fitted with a single exponential function to estimate τ_{deact}, which has been plotted *versus* repolarization voltage for wild type (■) or F448L (●) expressed alone and for wild type and F448L expressed at a 1:1 ratio (□). Values are provided as mean ± SEM, $n \geq 9$. All τ_{deact} values differed significantly from wild type expressed alone, $P < 0.00001$ by one-way ANOVA followed by 2 sample *t* test.

the voltage dependence of opening in the hyperpolarized direction and dramatically slowing deactivation, whereas the R420H and R423H mutations suppress Kv3 current amplitude by a dominant negative mechanism (Waters *et al.* 2006; Figueroa *et al.* 2010). These results were puzzling given the clinical overlap between the R423H and F448L mutations and the distinct form of SCA13 generated by R420H.

A limited number of R420 or R423H subunits can assemble with wild type subunits to form active channels

In this study, we investigated the stoichiometry of the dominant negative effects of the R420H and R423H mutant subunits. We found that one R420H and at least one R423H subunit can assemble with wild type subunits to generate active, cell surface channels. These results were confirmed by a second, independent approach based on an inactivation-tagging strategy. We also showed that R423H subunits expressed alone at high levels are able to form active channels, albeit inefficiently. Although it seems unlikely that a significant number of R423H homotetramers would exist *in vivo*, these results further demonstrate that R423H subunits are compatible with channel activity.

Changes in Kv3.3 gating are correlated with SCA13 onset in early childhood

Our results support the conclusion that altering Kv3.3 gating contributes substantially to the early age of onset seen with the R423H and F448L mutations. Significantly, incorporation of R420H subunits into active channels had little effect on the functional properties of Kv3.3, whereas incorporation of R423H subunits shifted activation to hyperpolarized voltages and slowed channel opening and closing. Importantly, R423H and F448L, which cause the infant-onset form of SCA13, had similar effects on channel gating. The voltage dependence and kinetics of activation were strikingly similar in channels formed from 1:1 mixtures of wild type and R423H, or wild type and F448L subunits (Table 1). In addition, both mutations slowed channel closing, although the effect of F488L was substantially larger than R423H. Despite this difference, the available clinical data suggest that the severity of SCA13 caused by R423H or F448L is similar. This may reflect the fact that R423H affects Kv3.3 function by two mechanisms – dominant negative suppression of current amplitude and dominant gain of function changes in channel gating. Both effects may contribute to early disease onset in individuals with the R423H mutation. It is important to emphasize, however, that reducing current amplitude without altering gating is not sufficient to generate infant-onset disease, as shown by the R420H mutation (Waters *et al.* 2006; Figueroa *et al.* 2010).

Co-expressing wild type and mutant subunits at a 1:1 ratio mimics the genotype of SCA13 patients. However, *in vivo*, mutant Kv3.3 subunits may co-assemble with wild type subunits of other Kv3 family members if they are expressed in the same cell (Weiser *et al.* 1994; Martina *et al.* 2007). As a result, the actual ratio of wild type to mutant subunits *in vivo* is unknown and likely to vary in different types of neurons depending on what complement of *KCNC* genes is expressed.

Functional phenotypes identified in oocytes are relevant to the effects of SCA13 mutations *in vivo*

Our previous work strongly supports the idea that changes in Kv3.3 channel function, initially identified using the oocyte expression system, are responsible for the effects of SCA13 mutations *in vivo* (Issa *et al.* 2011). We have shown that the adult-onset R420H mutation reduces the capacity for sustained, repetitive firing in Kv3.3-expressing neurons in zebrafish (Issa *et al.* 2011). Spike failure results directly from the subfamily-specific dominant negative effect of the R420H subunit on Kv3 current amplitude (Waters *et al.* 2006). R420H significantly decreases the amplitude of outward currents in neurons, but has no effect on the amplitude of inward currents. The correlation between decreased K^+ current amplitude and reduced neuronal excitability confirms that the R420H subunit specifically suppresses Kv3 channel activity, as expected (Waters *et al.* 2006; Issa *et al.* 2011). In most instances, decreasing K^+ current amplitude would be expected to increase neuronal excitability. However, this is not the case for Kv3 channels. Kv3 channels enhance excitability by opening rapidly during action potentials, promoting fast spike repolarization and rapid recovery of Na^+ channel inactivation (Rudy & McBain, 2001). When Kv3 current amplitude is reduced, trains of action potentials end prematurely due to the accumulation of Na^+ channel inactivation. These findings indicate that functional analysis in oocytes yields results that are relevant to the effects of SCA13 mutations in neurons *in vivo*.

The finding that R420H reduces the capacity for sustained firing is consistent with our proposal that changes in excitability underlie SCA13 (Issa *et al.* 2011). The R423H and F448L mutations are also expected to alter action potential firing. Activation of Kv3 channels at more negative voltages and, in the case of F448L, slower deactivation kinetics, would modify spike frequency during repetitive firing. *A priori*, it seems unlikely that R423H and F448L would impair a neuron's capacity for sustained firing. Therefore, the infant-onset and adult-onset mutations are expected to alter excitability

in distinct ways. This may contribute to the different ages at which disease emerges in the two forms of SCA13.

Novel gating properties of Kv3 channels contribute to normal cerebellar development

Our results suggest that the novel gating properties of Kv3.3 channels play an important role in cerebellar development. We found a strong correlation between changes in Kv3.3 channel gating and infant-onset SCA13. In a 5 year old with the F448L mutation, the cerebellum is severely shrunken (Herman-Bert *et al.* 2000). A small cerebellum has also been reported in a 3 year old with the R423H mutation (Figueroa *et al.* 2011). These findings raise the possibility that the R423H and F448L mutations increase the susceptibility of Kv3.3-expressing neurons to cell death during development. Cell death is a normal part of brain development, serving to refine synaptic connections, but would no doubt become pathological at excessive levels (Kuan *et al.* 2000).

R420H and R423H subunits did not generate detectable gating pore currents

Several human channelopathies result from mutations of arginine residues in the S4 segment of voltage-gated ion channels (Sokolov *et al.* 2007; Cannon, 2010; Catterall, 2010). It has been proposed that these mutations generate pathological gating pore currents that underlie the disease phenotypes (Sokolov *et al.* 2007; Catterall, 2010). We were unable to detect voltage- and/or pH-dependent currents after expressing R420H or R423H subunits containing the W495F mutation to block conduction through the central pore. However, gating pore currents can be extremely small in amplitude (Struyk & Cannon, 2007). Therefore, we cannot rule out the possibility that the R420H or R423H mutations generate tiny gating pore currents that were not detected in our experiments.

The apparent lack of gating pore currents in R420H and R423H is perhaps not surprising. Cell surface expression is required to detect currents flowing through the voltage sensor domain. Hypokalaemic periodic paralysis mutations in Nav1.4 generate small-amplitude gating pore currents. However, the mutant channels conduct robust Na^+ currents through the central pore, indicating that the mutant proteins traffic efficiently to the plasma membrane (Sokolov *et al.* 2007; Struyk & Cannon 2007). This may reflect the fact that the mutations are present in only one of the four pseudosubunits of the Na^+ channel protein. In contrast, K^+ channels comprise four separate subunits. R420H tetramers are non-functional, whereas R423H forms active tetramers very inefficiently. (For comparison, it is worth noting that the Shaker channel from *Drosophila* is, in general, more tolerant of mutations than many mammalian K^+ channels. The analogous mutations in Shaker are robustly active (Starace *et al.* 1997; Starace & Bezanilla, 2001).) A likely possibility is that the Kv3.3 R420H or R423H mutations result in endoplasmic reticulum retention of all or most of the channel protein when the mutant subunits are expressed alone. Indeed, when the mutant proteins are expressed with wild type, endoplasmic reticulum retention of co-assembled wild type subunits may be the mechanism of dominant negative suppression, as we have previously shown in Shaker channels (Schulteis *et al.* 1998). If so, the R420H and R423H proteins would reach the cell surface in limited numbers only by assembling with wild type subunits into active channels. Thus, even if the mutations did make the voltage sensor leaky, there may be too little mutant protein at the plasma membrane to generate gating pore currents that contribute to the disease phenotype.

References

Baukrowitz T & Yellen G (1995). Modulation of K^+ current by frequency and external $[K^+]$: a tale of two inactivation mechanisms. *Neuron* **15**, 951–960.

Blaine JT & Ribera AB (1998). Heteromultimeric potassium channels formed by members of the Kv2 subfamily. *J Neurosci* **18**, 9585–9593.

Cannon SC (2010). Voltage-sensor mutations in channelopathies of skeletal muscle. *J Physiol* **588**, 1887–1895.

Catterall WA (2010). Ion channel voltage sensors: structure, function, and pathophysiology. *Neuron* **67**, 915–928.

Desai R, Kronengold J, Mei J, Forman SA & Kaczmarek LK (2008). Protein kinase C modulates inactivation of Kv3.3 channels. *J Biol Chem* **283**, 22283–22294.

Figueroa KP, Minassian NA, Stevanin G, Waters M, Garibyan V, Forlani S *et al.* (2010). KCNC3: Phenotype, mutations, channel biophysics – a study of 260 familial ataxia patients. *Hum Mutat* **31**, 191–196.

Figueroa KP, Water MF, Garibyan V, Bird TD, Gomez CM, Ranum LPW *et al.* (2011). Frequency of KCNC3 DNA variants as causes of spinocerebellar ataxia 13 (SCA13). *PLoS ONE* **6**, e17811.

Herman-Bert A, Stevanin G, Netter J, Rascol O, Brassat D, Calvas P *et al.* (2000). Mapping of spinocerebellar ataxia 13 to chromosome 19q13.3-q13.4 in a family with autosomal dominant cerebellar ataxia and mental retardation. *Am J Hum Genet* **67**, 229–235.

Hoshi T, Zagotta WN & Aldrich RW (1991). Two types of inactivation in Shaker K^+ channels: effects of alterations in the carboxy-terminal region. *Neuron* **7**, 547–556.

Issa FA, Mazzochi C, Mock AF & Papazian DM (2011). Spinocerebellar ataxia type 13 mutant potassium channel alters neuronal excitability and causes locomotor deficits in zebrafish. *J Neurosci* **31**, 6831–6841.

Kuan C-Y, Roth KA, Flavell RA & Rakic P (2000). Mechanisms of programmed cell death in the developing brain. *Trends Neurosci* **23**, 291–297.

MacKinnon R (1991). Determination of the subunit stoichiometry of a voltage-activated potassium channel. *Nature* **350**, 232–235.

MacKinnon R, Aldrich RW & Lee AW (1993). Functional stoichiometry of Shaker potassium channel inactivation. *Science* **262**, 757–759.

Manganas LN & Trimmer JS (2000). Subunit composition determines Kv1 potassium channel surface expression. *J Biol Chem* **275**, 29685–29693.

Martina M, Metz AE & Bean BP (2007). Voltage-dependent potassium currents during fast spikes of rat cerebellar Purkinje neurons: inhibition by BDS-1 toxin. *J Neurophysiol* **97**, 563–571.

Mock AF, Richardson JL, Hsieh J-Y, Rinetti G & Papazian DM (2010). Functional effects of spinocerebellar ataxia type 13 mutations are conserved in zebrafish Kv3.3 channels. *BMC Neurosci* **11**, 99.

Myers MP, Khanna R, Lee EJ & Papazian DM (2004). Voltage sensor mutations differentially target misfolded K^+ channel subunits to proteasomal and non-proteasomal disposal pathways. *FEBS Lett* **568**, 110–116.

Papazian DM, Timpe LC, Jan YN & Jan LY (1991). Alteration of voltage dependence of Shaker potassium channel by mutations in the S4 sequence. *Nature* **349**, 205–310.

Perozo E, MacKinnon R, Bezanilla F & Stefani E (1993). Gating currents from a nonconducting mutant reveal open-closed conformations in Shaker K^+ channels. *Neuron* **11**, 353–358.

Rae JL & Shepard AR (2000). Kv3.3 potassium channels in lens epithelium and corneal endothelium. *Exp Eye Res* **70**, 339–348.

Rudy B & McBain CJ (2001). Kv3 channels: voltage-gated K^+ channels designed for high-frequency repetitive firing. *Trends Neurosci* **24**, 517–526.

Schulteis CT, Nagaya N & Papazian DM (1998). Subunit folding and assembly steps are interspersed during Shaker potassium channel biogenesis. *J Biol Chem* **273**, 26210–26217.

Sokolov S, Scheuer T & Catterall WA (2007). Gating pore current in an inherited ion channelopathy. *Nature* **446**, 76–78.

Starace DM & Bezanilla F (2001). Histidine scanning mutagenesis of basic residues of the S4 segment of the Shaker K^+ channel. *J Gen Physiol* **117**, 469–490.

Starace DM, Stefani E & Bezanilla F (1997). Voltage-dependent proton transport by the voltage sensor of the Shaker K^+ channel. *Neuron* **19**, 1319–1327.

Struyk AF & Cannon SC (2007). A Na^+ channel mutation linked to hypokalemic periodic paralysis exposes a proton-selective gating pore. *J Gen Physiol* **130**, 11–20.

Swenson RP & Armstrong CM (1981). K^+ channels close more slowly in the presence of external K^+ and Rb^+. *Nature* **291**, 427–429.

Timpe LC, Schwarz TL, Tempel BL, Papazian DM, Jan YN & Jan LY (1988). Expression of functional potassium channels from *Shaker* cDNA in *Xenopus* oocytes. *Nature* **331**, 143–145.

Tiwari-Woodruff SK, Schulteis CT, Mock AF & Papazian DM (1997). Electrostatic interactions between transmembrane segments mediate folding of Shaker K^+ channel subunits. *Biophys J* **72**, 1489–1500.

Waters MF, Minassian NA, Stevanin G, Figueroa KP, Bannister JPA, Nolte D *et al.* (2006). Mutations in the voltage-gated potassium channel KCNC3 cause degenerative and developmental CNS phenotypes. *Nat Genet* **38**, 447–451.

Weiser M, Vega-Saenz de Miera E, Kentros C, Moreno H, Franzen L, Hillman D *et al.* (1994). Differential expression of Shaw-related K^+ channels in the rat central nervous system. *J Neurosci* **14**, 949–972.

Author's present address

N.A. Minassian: Johnson & Johnson, 3210 Merryfield Row, San Diego, CA 92121, USA.

Author contributions

D.M.P. conceived of and directed the study; N.A.M. and M.-C.A.L. performed experiments and analysed data; D.M.P. wrote the paper with input from N.A.M. and M.-C.A.L. All authors approved the final version.

Acknowledgements

We are grateful to Dr Joanna Jen and Jui-Yi Hsieh for comments on the manuscript. We thank Allan Mock for excellent technical assistance. This work was supported by NIH grant R01 NS058500 to D.M.P. N.A.M. was partially supported by NIH training grant T32NS007449 (PI: M.F. Chesselet) and the Jennifer S. Buchwald Endowment.